PLANT SCIENCE TODAY
Vol 13(2): 1-8
https://doi.org/10.14719/pst.13145

eISSN 2348-1900

RESEARCH ARTICLE

# *Tinospora cordifolia* GCMS profiling and cytotoxic effect on HCT 116- *in vitro* assay: Anticancer phytochemical screening

**Manimozhi S & Sumathi V***

[1]Department of Microbiology, Annamalai University, Chidambaram, Tamil Nadu 608002, India.

*Correspondence email - sumathikarthidd@gmail.com

Received: 10 December 2025; Accepted: 25 February 2026; Available online: Version 1.0: 20 April 2026; Version 2.0: 27 April 2026

**Cite this article:** Manimozhi S, Sumathi V. *Tinospora cordifolia* GCMS profiling and cytotoxic effect on HCT 116- *in vitro* assay: Anticancer phytochemical screening. Plant Science Today. 2026; 13(2): 1-8. https://doi.org/10.14719/pst.13145

## Abstract

An assessment of ethylacetate extract of *Tinospora cordifolia* extract (TCE) antibacterial, antioxidant and cytotoxicity on HCT116 properties were undertaken in light of its possible application as an anticancer agent against colon cancer. Compounds from the stem were Soxhlet extracted with ethyl acetate and identified through GCMS. Antibacterial activity by disc diffusion and conventional *in vitro* antioxidant assays was performed. The cytotoxicity of the extract was studied by MTT assay. The data of the GC–MS profile highlights 20 diverse chemical compounds. The extract exhibited broad-spectrum antibacterial activity on clinical pathogens with relative inhibition of 83 to 107 % and the zone of inhibition was found to be concentration-dependent. The antioxidant assay of the extract showed the strongest DPPH scavenging with an $IC_{50}$ value of 12.07 µg/mL, which, although higher, showed promising free radical scavenging and the $IC_{50}$ values were 331.97, 12.078 and 67.867 µg/mL on OH scavenging, DPPH and metal chelation. The effect of the extract on the viability of HCT116 colorectal carcinoma cells showed induced cell death significantly at higher concentration and the calculated $IC_{50}$ value was 359 µg/mL. Morphological examination and apoptosis assays further confirmed that cell death was predominantly apoptotic nature in cancerous cells. The molecular docking of compounds 2-Fluoro-3-trifluoromethylbenzoic acid from the extract was found to be strongest binding affinity and non-toxic drug likeness, identified as a promising new anticancer compound.

**Keywords:** antibacterial; anticancer; antioxidant; GC-MS; HCT116; tinospora

## Introduction

Colorectal cancer (CRC) is among the most frequently reported cancers in the world. CRC is now the second most prevalent cancer diagnosed in women and the third in men, according to Global Cancer Statistics (1). There were over 900000 colorectal cancer deaths and 1.9 million new cases globally in 2022. Phytochemical Promising opportunities for the development of safer anticancer medications to overcome the adverse effects of chemotherapy remain limited. As a result, research on *Tinospora cordifolia* significant medicinal herb in the Ayurvedic medicinal system, has been studied for alternative biomedical therapy. The only member of the Tinospora genus had demonstrated anti-carcinogenic qualities was *T.cordifolia* even less explored (2). Ayurvedic medicine uses *T.cordifolia* (Willd.) as a well-known herb. It is also known as Rasayana (to purify the blood) and Amrita (to bring the dead back to life) (3). It is from the tropical part of India and can grow up to 500 m high in temperatures between 25 and 45 °C (4). *Tinospora* spp. possess numerous beneficial medicinal properties, including antioxidant, antimicrobial, anti-diabetic, anti-ageing and cytotoxic activities (5). *T. cordifolia* is a rich source of bitter alkaloids, including tinosporin, tinosporic acid and tinosporol, which have been shown to have medicinal effects (6). *T. cordifolia* has been scientifically documented to possess antidiabetic, hepatoprotective and immunomodulatory properties (7). Berberine (BBR), a secondary metabolite of this plant, has been employed in the treatment of cancer across various cell types (8). The antibacterial properties of *T. cordifolia* stem extracts are effective against microbial infections caused by urinary pathogens, including *Klebsiella pneumoniae* and *Pseudomonas aeruginosa* (9). Oxidative stress occurs when the body's defences against oxidative damage and the production of reactive oxygen species (ROS) are not in balance. Consequently, the investigation of natural antioxidants, including those found in *T. cordifolia*, presents significant potential for preventive and therapeutic applications (10). The objective of the present study is to examine the antibacterial and cytotoxic properties of an ethyl acetate extract of *T. cordifolia* stem through an *in vitro* methodology.

## Materials and Methods

### Plant material collection and authentication

The Plant sample of *Tinospora cordifolia* species was collected in the Cuddalore district (11.684689/79.721434), during June 2024. A herbarium was prepared and authenticated by a botanist at the Department of Botany, Annamalai University, Chidambaram.

### Preparation and extraction of phytochemicals

The plant material stem (250 g) was dried well in the shade for several days. The dried sample was ground well in a mechanical grinder. The powder was sieved to get a uniform particle size and a fine powder 220 g was obtained. 100 g of fine powder was packed

into a 25 x 80 mm porous extraction thimble and assembled with the extractor unit. The extraction was done by the Soxhlet method as described in the previous method. The setup was mounted on round bottom flask containing 250 mL of ethyl acetate. The extraction begins with heating the solvent phase at 50 °C on a heating mantle for 3 hr. A condenser set up was connected and maintained with continuous cold water circulation to avoid overheating. The condensed ethylacetate phase form bottom flask was collected and dried under a desiccator with silica gel. 10 mg of dried sample resuspended in 10 mL same solvent and used for GCMS.

## Antibacterial activity of the extract

The ethyl acetate extracts of *T. cordifolia* were used for disc diffusion antibacterial assay as per ICMR guidelines (12). Muller Hinton agar plates were used and 24 hr old bacterial culture was swabbed over the agar surface with a sterile swab. Sterile diss preloaded with extract (10 mg/mL) at different concentrations, such as 25µg, 50µg, 75 and 100 µg were placed on plates with known standard and negative control. All inoculated plates were kept under incubation at 37 °C for 24 hr. The plates were observed for zones of inhibition after 24 hr and compared with Gentamycin standard (30 µg) and the relative inhibitory zone diameter (RIZD) was calculated using the following equation 1.

% RIZD = Diameter of test zone / Diameter of reference zone × 100 (Eqn. 1)

## DPPH antioxidant assay

The free radicals of the stem extract of *T. cordifolia* were determined by the DPPH (1,1-diphenyl-2-picryl hydrazyl) technique. A total of 20 mg of DPPH was dissolved in 20 mL of ethyl acetate to make the stock solution (13). The assay was performed by the microtiter plate method with a final volume of 500 µL. 200 µL of ethyl acetate, 200 µL of DPPH and 100 µL of the sample at different concentration was added and incubated in dark conditions for 5 min. Ascorbic acid is used as the standard. The absorbance was taken at 517 nm. The following equation was used to compute the DPPH scavenging effect of antioxidants.

Percentage of inhibition = $A_0$-$A_1$/$A_0$ × 100 (Eqn. 2)

Where, $A_0$=The absorbance of the control, $A_1$=The absorbance of the sample.

## Metal chelation assay

Metal chelating activity was measured as described previously in the literature (14). The reaction mixture was prepared by adding 0.1 mM $FeSO_4$ (0.2 mL) and 0.25 mM ferrozine (0.4 mL). Subsequently, 0.2 mL of the test compound in ethyl acetate was added at different concentrations. After incubating at room temperature for 10 min, the absorbance of the mixture was recorded at 562 nm. EDTA used as 'standard'. Chelating activity was calculated using the following Eqn:

Metal chelating activity = $(A_{control} - A_{sample})/A_{control} \times 100$ (Eqn. 3)

## Hydrogen peroxide scavenging activity

The radical scavenging activity of individual extracts was determined using the $H_2O_2$ method. Briefly, 2 mL of test solution in ethyl acetate was added to 4.0 mL of hydrogen peroxide ($H_2O_2$) (20 mM) solution in phosphate buffer (pH 7.4) (15). After 10 min, the absorbance was measured at λmax 230 nm against the phosphate buffer blank solution. The percentage scavenging of $H_2O_2$ was calculated using the equation:

% scavenging of $H_2O_2 = [(A_0 - A_1)/A_0] \times 100$, (Eqn. 4)

Where, $A_0$ = absorbance of the control, $A_1$ = absorbance of the test extracts.

## Cytotoxicity of the extract on HCT116

Cell culture: NCCS, Pune, provided the triple human colorectal carcinoma cell line (HCT-116). In addition to 10 % fetal bovine serum (Gibco), 1 % Sodium Bicarbonate and 1 % Sodium Pyruvate (HiMedia), the cells were cultivated in Dulbecco's modified eagle's Medium (DMEM, HiMedia). For subsequent tests, the cells were kept at 37 °C in a humidified environment with 5 % $CO_2$.

## Viability analysis by 3-(4, 5-dimethylthiazol-2-yl)-2,5-diphenyltetrazolium bromide (MTT)

The sample drug's efficient cytotoxic concentration was examined using MTT (Tetrazolium salt; HiMedia). A 96-well plate was seeded with 1 × 104 HCT116 cells per well (16). After that, the cells were cultured for a full day. The cells were incubated for an additional 24 hr after being treated with a sample drug (Crude Extract) at a dose of 100–1000 µg/mL. The cells were cultured for five hours, the media was carefully withdrawn and the formazan crystals were dissolved in 100 µL of dimethyl sulfoxide (DMSO) for thirty minutes after 100 µL of complete media containing MTT (0.5 mg/mL) was added to each well. After that, the absorbance was measured at 570 and 650 nm using a microplate reader and the $IC_{50}$ value was determined.

## Inhibition of cyclin-dependent kinase 4 (CDK4) by phytochemical *in silico* analysis

### Protein preparation

The molecular docking target CDK4 was retrieved from the protein data bank (PDB ID:7SJ3) due to its critical role in controlling cell cycle progression from $G_1$ to S phase. The unwanted co-crystallised ligand and water molecules were removed and the enzyme was prepared using the QuickPrep tool module in the MOE program, saved as pdb and converted to PDBQT format by Autodock vina. AutoDock Tools was employed to set the size and the centre of the grid box. Partially charged atoms were allocated partial charges and polar hydrogen was added to create a protonation state at physiological pH.

### Ligand preparation

The phytochemical three-dimensional (3D) structures were obtained from the PubChem database, which is accessible via the NCBI website using the UCSF Chimaera program (v.1.14). Smiles were used to build a structure and were optimised.

### Molecular docking

The ligand protein binding affinity was assessed by calculating the scoring function based on geometry. The AutoDock Vina feature in the UCSF Chimaera program version 1.14 was utilised to carry out the molecular docking study (16). View Dock was used to investigate binding affinity. Using discovery studio 2020 Client, the final results were examined and displayed. The grid box at the active site was prepared and the ligand was positioned. The autodock was performed using the standard operating procedure.

### Absorption, distribution, metabolism and excretion (ADME) and toxicity prediction

The Lipinski rule was used to further the drug likeness of the selected ligand. Swiss ADME, ligand pharmacokinetic profile (ADME) was performed and toxicity predictions were performed (17). The Simplified Molecular Input Line Entry System (SMILES) notations allowed for the analysis of the toxicological characteristics of ligands.

## Results and Discussion

### Compound analysis of ethyl acetate extract

The extract's GC–MS analysis identified a variety of bioactive chemicals, which are listed in Table 1. Twenty peaks in all were found to represent several kinds of chemicals, such as complex bicyclic derivatives, siloxanes, organic acids, esters and heterocycles (Fig. 1). Hexanedioic acid, bis(2-ethylhexyl) ester (39.59 % peak area; RT 32.884 min), a phthalate derivative that is frequently reported as a plasticiser but is also linked to antibacterial and antioxidant qualities, was the most prevalent component. 1,2-Benzenedicarboxylic acid, dicyclohexyl ester (9.70 %; RT 24.844 min), cyclohexasiloxane, dodecamethyl (11.38 %; RT 13.876 min) and 1,3-diphenyl-1-((trimethylsilyl)oxy)-1(Z)-heptene (5.69 %; RT 17.486 min) were additional significant elements. Benzoic acid derivatives (2.45 %; RT 9.958 min), nonanoic acid methyl ester (3.63–3.53 %), 2-keto-butyric acid (1.28 %; RT 6.83 min) and 2(E)-tert-butyladamantan-2,4-diol (2.83 %) are minor molecules that add to the extract's biochemical complexity. Alkaloid-like structures were also found in several heterocyclic compounds that contained nitrogen and oxygen, such as Furo [2, 3-c] pyridine, 2, 3-dihydro-2, 7-dimethyl- and 12-azabicyclo (9.2.1) tetradeca-1(14)-ene-13-one (multiple peaks, total >5 %). The existence of siloxane derivatives and phthalate esters, which are occasionally regarded as pollutants. The extract's reported bioassays are consistent with the well-documented antibacterial, antifungal and antioxidant properties of compounds such as phthalates, nonanoic acid esters and benzoic acid derivatives (18). Specifically, the identification of aromatic derivatives and esters such as hexanedioic acid bis(2-ethylhexyl) ester indicates that these metabolites might work in concert to enhance the extract's antibacterial and free radical scavenging properties (19). Because of the widespread use of phthalates and siloxanes as well as their volatile properties, these compounds are present in considerable quantities across the world, especially indoors (20).

### Antioxidant potential of the extract

The antioxidant potential of the extract at concentrations ranging from 25–100 µg/mL is given in Table 2. The free radical scavenging activity increased in a dose-dependent manner. Hydroxyl scavenging was recorded from 33.00 ± 1.00 to 72.00 ± 1.00 % between 25 and 100 µg/mL, with an $IC_{50}$ value of 331.97 µg/mL. The DPPH radical scavenging activity was greater, with scavenging activity of 62.04 ± 0.00 and 82.31 ± 0.00 % at 25 and 100 µg/mL showed a comparatively lower $IC_{50}$ of 12.078 µg/mL. The metal chelation assay of the extract exhibited moderate chelating ability, ranging from 39.69 ± 1.00 at 25 µg/mL and reaching a maximum of

**Table 1.** Phytochemicals identified from GCMS spectrum

| Peak | RT | Area % | Name |
|---|---|---|---|
| 1 | 6.83 | 1.28 | 2-Keto-butyric-acid |
| 2 | 9.958 | 2.45 | Benzoic acid, 2,6-bis(trimethylsiloxy)-, trimethylsilyl ester |
| 3 | 13.876 | 11.38 | Cyclohexasiloxane, dodecamethyl- |
| 4 | 17.486 | 5.69 | 1,3-Diphenyl-1-((trimethylsilyl)oxy)-1(z)-heptene |
| 5 | 20.718 | 2.99 | Tri-o-trimethylsilyl, n-trifluoroacetyl derivative of terbutaline |
| 6 | 23.512 | 0.98 | Phosphonous dibromide, [2,2,2-trifluoro-1-(trifluoromethyl)-1-[(trimethylsilyl)oxy]ethyl]- |
| 7 | 24.844 | 9.7 | 1,2-Benzenedicarboxylic acid, dicyclohexyl ester |
| 8 | 25.955 | 3.63 | Nonanoic acid, methyl ester |
| 9 | 26.43 | 2.25 | Furo[2,3-c]pyridine, 2,3-dihydro-2,7-dimethyl- |
| 10 | 29.132 | 3.53 | Nonanoic acid, methyl ester |
| 11 | 32.884 | 39.59 | Hexanedioic acid, bis(2-ethylhexyl) ester |
| 12 | 34.76 | 2.83 | 2(E)-Tert-butyladamantan-2(a),4(a)-diol |
| 13 | 38.255 | 2.69 | 1-Hydroxyspiro[5.12]octadecan-7-one |
| 14 | 38.295 | 2.63 | 2-(N-Methylpyrrolyl) furoate |
| 15 | 38.35 | 1.07 | 12-Azabicyclo(9.2.1)tetradeca-1(14)-ene-13-one |
| 16 | 38.381 | 1.22 | 1,5,7-Trimethyl-3-oxo-2-oxabicyclo[4.2.0]oct-4-ene-(endo)-7-carbonitrile |
| 17 | 38.405 | 1.33 | 2-Fluoro-3-trifluoromethylbenzoic acid, heptyl ester |
| 18 | 38.44 | 2.45 | 12-Azabicyclo(9.2.1) tetradeca-1(14)-ene-13-one |
| 19 | 38.491 | 1.79 | 12-Azabicyclo(9.2.1)tetradeca-1(14)-ene-13-one |
| 20 | 39.507 | 0.51 | Cesium trimethylfluoro) aluminate |

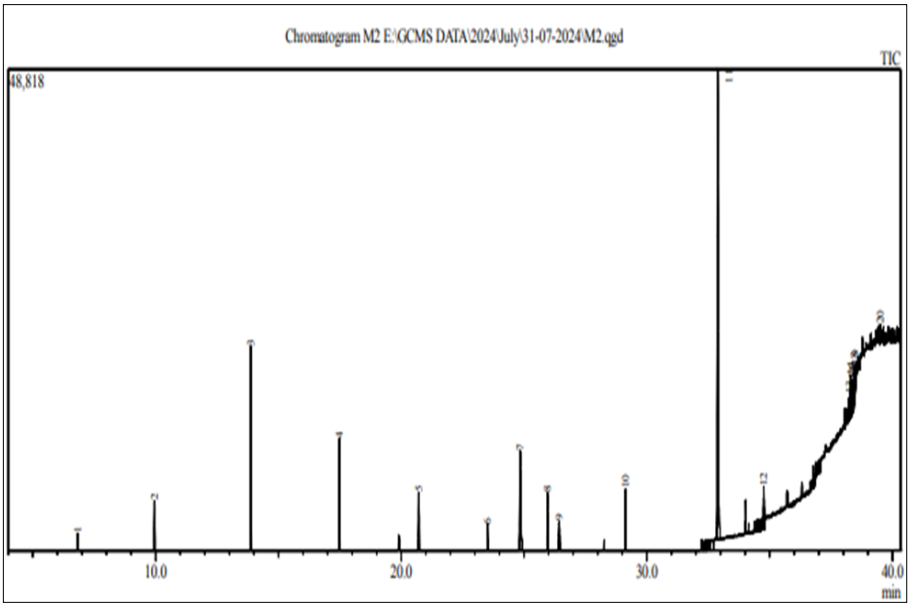


**Fig. 1.** Retention time of peaks eluted from ethyl acetate extract.

64.16 ± 0.32 % at 100 µg/mL with an $IC_{50}$ value of 67.86 µg/mL. These results indicate that the extract exerts considerable free radical scavenging ability. *Tinospora cordifolia* stem extract antioxidant capacity correlates with the recent finding of DPPH activity (21). The hydroxyl radical antioxidant capacity of the suggests a strong ability to neutralise hydroxyl radicals at increased concentrations. The observed activity may be attributed to secondary metabolites such as tannins and polyphenolic compounds, which possess hydroxyl and carbonyl groups capable of binding metal ions. The strong dose-dependent inhibition highlights the presence of efficient free radical quenchers such as phenolics and flavonoids. *Tinospora cordifolia* aqueous extract was earlier reported as having better antioxidative properties than the solvent (22). Likewise, ethanol extract and n-butanol fractions of *Tinospora* were reported as superior radical scavenging in DPPH and metal chelation in earlier studies, in contrast to ethylacetate extract (23).

## Antibacterial activity

The antibacterial activity of the extract was evaluated against seven bacterial pathogens and compared with a standard antibiotic (Table 3). The extract exhibited broad-spectrum inhibitory effects with zones of inhibition ranging from 19.33 ± 0.57 mm to 21.66 ± 1.52 mm. The maximum inhibition was observed against *K. pneumoniae* (21.66 ± 1.52 mm), followed closely by *Proteus mirabilis* (21.33 ± 1.15 mm) and *P. aeruginosa* (20.66 ± 0.57 mm). Significant activity was noted against *Escherichia coli* (20.33 ± 1.52 mm), *Enterococcus faecalis* (20.00 ± 1.00 mm) and *Staphylococcus aureus* (19.33 ± 0.57 mm). Interestingly, the extract displayed greater activity against *Bacillus* sp. (19.33 ± 1.15 mm) compared to the standard drug (18.00 ± 0.00 mm), indicating selective potency.

The extract showed strong and consistent antibacterial action, despite the fact that the conventional antibiotic regularly produced slightly bigger inhibition zones. The absence of inhibition with the negative control (nc) demonstrated that the extract was the only source of the activity. The information was discovered (24). Additionally, it was noted that *Tinospora cordifolia* may help fight clinical infections' medication resistance (25). With values ranging from 83.11 % to 107.47 % of the standard, the relative inhibitory zone diameter (RIZD) study demonstrated the extract's strong antibacterial activity against every tested pathogen (Fig. 2). The extract beat the conventional antibiotic against *Bacillus* sp., which showed the highest relative activity (107.30 %). Additionally, strong inhibitory effects were noted against *E. faecalis* (88.23 %), *P. aeruginosa* (96.87 %) and *S. aureus* (95.08 %). *Proteus mirabilis* (83.11 %), *K. pneumoniae* (85.52 %) and *E. coli* (87.14 %) all showed moderate relative activity. These results demonstrate that the extract has broad-spectrum antibacterial activity, sometimes outperforming conventional medication.

## Cytotoxic effect of the extract on HCT116

Fig. 3a represents the cytotoxicity curve for HCT116 cells treated with compound extract at different concentrations (100–1000 µg/ml). The percentage of viability were calculated as 87.571 ± 7.19 ≥84.54 ± 2.7 ≥77.20 ± 6.07 ≥28.94 ± 1.85 ≥20.00 ± 3.06 ≥18.53 ± 1.09 ≥ 12.38 ± 2.61≥7.95 ± 0.66≥6.66 ± 1.33 percentage among 100-1000 µg /mL. The half-maximal inhibitory concentration ($IC_{50}$), where 50 % cell viability remains, was recorded from does response curve and calculated as 359 µg/mL (Fig. 3b. Compound M2 induces apoptosis in HCT116 cells in a dose-dependent manner, with the majority of cell death attributable to programmed cell death rather than necrosis. This aligns with cytotoxicity data ($IC_{50}$ ≈ 359 µg/ml), showing a strong apoptotic mechanism at higher concentrations. The higher $IC_{50}$ of crude phytochemicals may be reduced by purification of the compound. Cells exhibit membrane blebbing, cell shrinkage and chromatin condensation, which are hallmark features of apoptosis. Detached, rounded cells and apoptotic bodies are visible compared to the intact morphology of control cells (Fig. 4). Necrotic cells are relatively few, suggesting cell death is mainly apoptotic rather than necrotic. The results are concurrent with the findings in the cytotoxic effect of *T. cordifolia* on Oral colon cells (26). Research reported the anticancer activity of alkaloid palmatine derived from *Tinospora cordifolia* (27).

## Molecular docking and *Pharmacokinetics ADMET* of the active compound

The ADME/T profile of selected GC–MS identified compounds was evaluated to assess their drug-likeness and pharmacokinetic properties and compared with standard (Table 4). Both compounds satisfied Lipinski's rule of five, indicating acceptable oral bioavailability. Furo[2,3-c] pyridine, 2,3-dihydro-2,7-dimethyl- exhibited a molecular weight of 149.08 Da, good solubility (log S = –1.417), moderate lipophilicity (log P = 1.77) and complete blood–brain barrier (BBB) penetration (1.0). In contrast, *2-Fluoro-3-trifluoromethylbenzoic acid, heptyl ester* was heavier (306.12 Da), less soluble (log S = –5.941) and more lipophilic (log P = 5.182), with partial BBB penetration (0.799). Regarding absorption and distribution, both compounds showed low predicted human intestinal absorption (HIA = 0.0–0.001), but high plasma protein binding (PPB: 75.84 % and 99.23 %), which suggests strong binding affinity in systemic circulation. Both were predicted as P-glycoprotein substrates, although with low probabilities, indicating possible efflux by Pgp transporters. Metabolism predictions indicated that both molecules may act as CYP1A2 inhibitors, while *2-*

**Table 2.** Antioxidant activity of ethyl acetate extract

| Concentration (µg/mL) | Percentage of OH Scavenging | Percentage of DPPH | Percentage of metal chelation |
|---|---|---|---|
| 25 | 33 ± 1 | 62.04 ± 0 | 39.69 ± 1.004 |
| 50 | 47.66 ± 0.577 | 77.30 ± 0.34 | 41.77 ± 5.046 |
| 75 | 55.33 ± 0.577 | 80.62 ± 0 | 57.31 ± 1.059 |
| 100 | 72 ± 1 | 82.31 ± 0 | 64.16 ± 0.321 |
| $IC_{50}$µg | 331.97 | 12.078 | 67.867 |

**Table 3.** Antibacterial activity of ethyl acetate extract

| Organisms | Extract zone of inhibition (mm) | Standard zone of inhibition (mm) | Negative control |
|---|---|---|---|
| *K.pneumoniae* | 21.66 ± 1.52 | 25.33 ± 1.15 | 0 |
| *P.mirabilis* | 21.33 ± 1.15 | 25.66 ± 0.57 | 0 |
| *S.aureus* | 19.33 ± 0.57 | 20.33 ± 0.57 | 0 |
| *E.faecalis* | 20 ± 1 | 22.66 ± 1.15 | 0 |
| *P.aeruginosa* | 20.66 ± 0.57 | 21.33 ± 1.15 | 0 |
| *E.coli* | 20.33 ± 1.52 | 23.33 ± 1.15 | 0 |
| *Bacillus sp* | 1.15 | 18 ± 0 | 0 |

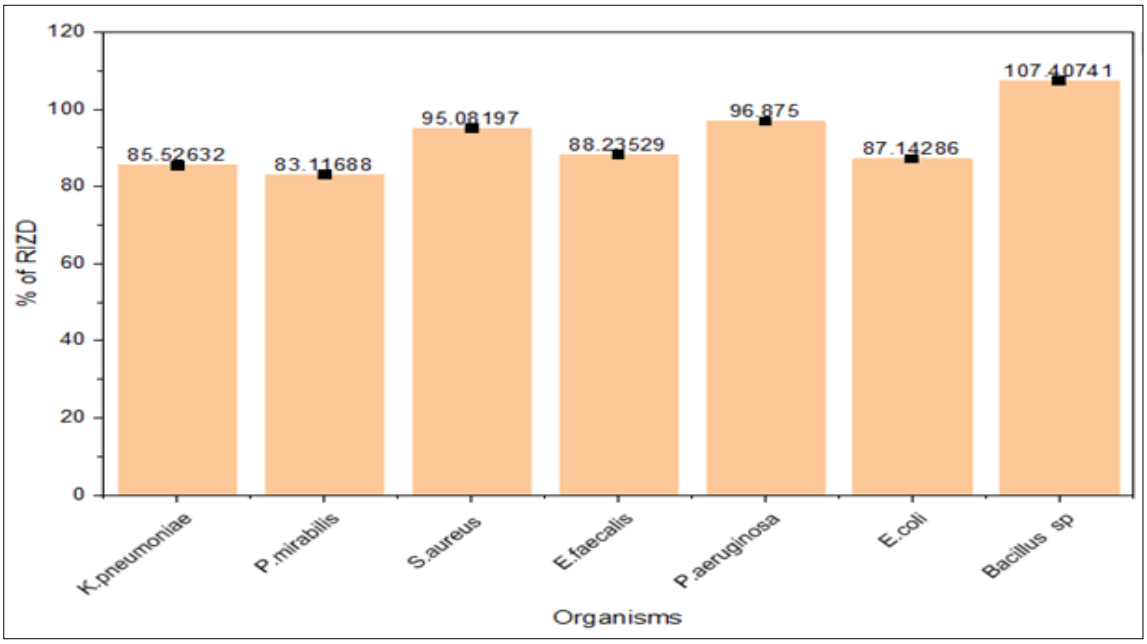


**Fig. 2.** Percentage of relative inhibition by extract.

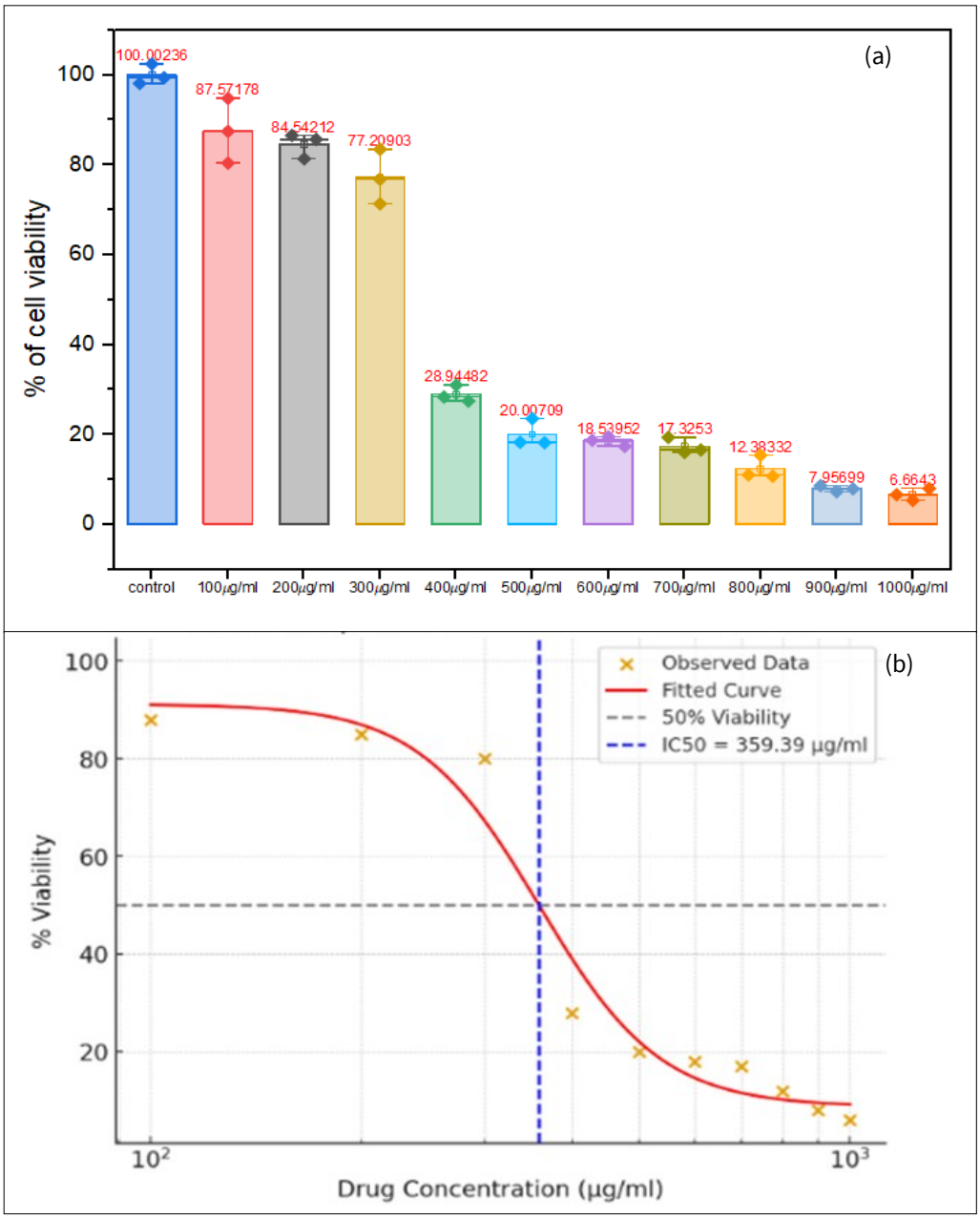


**Fig. 3.** Cytotoxicity of extract on HCT116 cell viability among different concentrations of extract: (a) Percentage of viability, (b) Does the response curve

*Fluoro-3-trifluoromethylbenzoic acid, heptyl ester*, additionally inhibited CYP2C19. These interactions suggest potential influence on hepatic drug metabolism. Both compounds were predicted to undergo clearance (CL = Yes) and exhibit extended half-life (T1/2 = Yes).

Toxicity profiling indicated mixed results on Furo[2,3-c] pyridine, which tested positive for AMES mutagenicity, hepatotoxicity, acute oral toxicity and carcinogenicity, whereas the heptyl ester derivative was non-mutagenic, non-carcinogenic and showed lower acute oral toxicity risk, though hepatotoxic potential remained. Overall, Furo[2,3-c] pyridine demonstrated favourable physicochemical and BBB penetration properties, but with concerning mutagenic and carcinogenic predictions. 2-Fluoro-3-trifluoromethylbenzoic acid, heptyl ester, displayed better drug-likeness, non-mutagenicity and non-carcinogenicity, although high plasma protein binding and CYP inhibition may limit its pharmacological safety. These findings suggest that while both compounds may contribute to the extract's bioactivity, careful consideration of toxicity is essential before therapeutic applications.

Table 5 shows the phytochemical-standard interaction and its binding affinity. According to docking studies, the target protein's interaction with Furo [2, 3-c] pyridine, 2, 3-dihydro-2 and 7-dimethyl was depicted on Fig. 4a. The binding cavity volume for 2AZ5 is 1263 Å$^3$. A moderate binding affinity is indicated by a binding score of -5.5 (in kcal/mol); a higher negative value typically suggests a greater projected binding. ASN. VAL, LEU and PHE were the residues that formed hydrogen bonds with the ligand. residues that participate in van der Waals or hydrophobic interactions. Fig. 4b showed the interaction between 2-fluoro-3-trifluoromethylbenzoic acid and heptyl ester with the target protein. The binding cavity volume for 2AZ5 is 396 Å$^3$. The binding affinity is estimated by the docking score, which is -6.9. Stronger anticipated binding between the ligand and the protein is typically indicated by more negative numbers. In addition to the hydrophobic contacts of Val, 2Leu, Gln and Phe, the residues Lys (2) and Thr were implicated in hydrogen bonding with the ligand. Previously, a series of furopyridine (PD) compounds were virtually screened using molecular docking to find strong EGFR inhibitors and synthetic derivatives of furopyridine as cytotoxic medicines against oesophageal cancer (28, 29). According to published research, *Callistemon lanceolatus* leaves contain anticancer chemicals such as 4-fluoro-2-trifluoromethylbenzoic acid (30). The potent standard doxorubicin showed a strong binding capacity for the target protein and the docking score of -9 kcal/mol (Fig 4c), suggesting a stable ligand–protein complex. The complex stabilisation within the active site was facilitated by the ligand's numerous interactions with important residues, such as Ile, Val, Thr, Asp and Glu. Through non-polar contacts, hydrophobic interactions were primarily seen with Ala, Leu and Glu residues, improving ligand accommodation inside the binding pocket. Furthermore, the ligand orientation was further stabilized and binding specificity was enhanced by a weak hydrogen bond with Val. Additionally, aromatic stacking (π-π interaction) with Phe residues was found, indicating strong electronic interactions that are known to contribute significantly to improved binding stability.

Doxorubicin molecular weight was 543.17 according to its ADME. Although the molecules tend to cling to one another because of the high number of hydrogen bond donors and acceptors , the membranes are less permeable to objects passing through (9, 12). The chemical is not soluble in water, according to logS (-2.69), although it has a significant lipid affinity, according to logP (1.76). Although it is anticipated that the human intestine would absorb a significant amount of this medication, it has been noted that because it does not pass the blood-brain barrier, it does not tend to disseminate much throughout the central nervous system. Its high P

**Table 4.** ADMET of compounds selected from GCMS

| S. No. | Properties | Furo[2,3-c]pyridine, 2,3-dihydro-2,7-dimethyl- | 2-Fluoro-3-trifluoromethylbenzoic acid, heptyl ester | Doxorubicin |
|---|---|---|---|---|
| 1 | Molecular Weight | 149.08 | 306.12 | 543.170 |
| 2 | nHA | 2.0 | 2.0 | 12 |
| 3 | nHD | 0.0 | 0.0 | 9 |
| 4 | logS | -1.417 | -5.941 | -2.690 |
| 5 | logP | 1.77 | 5.182 | 1.760 |
| 6 | HIA | 0.0 | 0.001 | **+++** |
| 7 | BBB Penetration | 1.0 | 0.799 | poor |
| 8 | Pgp-substrate | 0.019 (+) | 0.01(+) | 0.999 (+++) |
| 9 | Lipinski Rule | 0.0 | 0.0 | Rejected |
| 10 | F20 % | 0.002 | 0.067 | 0.024 |
| 11 | PPB | 75.841 | 99.239 | 91.288 % |
| 12 | CYP1A2 inhibitor | Yes | Yes | no |
| 13 | CYP2C19 inhibitor | No | Yes | no |
| 14 | CL | Moderate | High | high |
| 15 | T1/2 | Short | Long | long |
| 16 | AMES Toxicity | Positive | Negative | positive |
| 17 | Hepatotoxicity | Yes | Yes | positive |
| 18 | Rat Oral Acute Toxicity | Yes | No | negative |
| 19 | Carcinogencity | Yes | No | yes |

**Table 5.** Binding affinity of active compounds identified from the extract

| Compounds | Cavity volume (Å$^3$) | Vina score Kcal/mol | H bond | Other interaction |
|---|---|---|---|---|
| Furo [2, 3-c] pyridine, 2, 3-dihydro-2, 7-dimethyl- | 1263 | -5.5 | Asn | Val, Leu, Phe |
| 2-Fluoro-3-trifluoromethylbenzoic acid, heptyl ester | 1263 | -6.9 | Arg | Val, 2Leu, Gln, Phe |
| Doxorubicin | 892 | -9 | Ile, Val, Thr, Asp, Glu ,Thr | Hydrophobic Ala, Leu, Glu<br>Weak H bond:Val<br>Pi-pi:Phe |

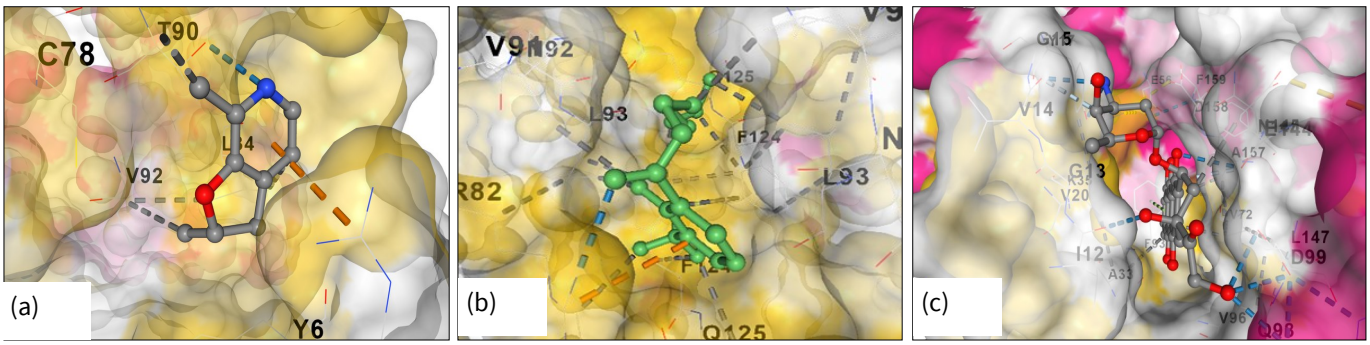


**Fig. 4.** Interaction of phytochemicals and standard with CDK4: (a) Furo [2, 3-c] pyridine, (b) 2-Fluoro-3-trifluoromethylbenzoic acid, (c) Doxorubicin

-gp substrate likelihood and Lipinski rule violation suggest that there may be issues with efflux limits and bioavailability. More systemic exposure is indicated by pharmacokinetic characteristics showing high clearance, a long half-life and substantial plasma protein binding (91.28 %). Non-inhibiting CYP1A2 and CYP2C19, the likelihood of certain medication interactions involving metabolism is decreased. Toxicological predictions show that AMES toxicity and hepatotoxicity are both positive, despite carcinogenicity being negative established safety concerns (31).

## Conclusion

The results show that the extract has broad-spectrum antibacterial and a wide range of free radical scavenging. The extract exhibited a significant cytotoxic effect on the HCT116 cancer cell line and the *in silico* prediction of active compound 2-Fluoro-3-trifluoromethylbenzoic acid, heptyl ester was effective, nontoxic and noncarcinogenic, unlike standard. These findings imply that the extract exhibited antiproliferation of cancerous cells, promising as an anticancer agent that causes concentration-specific apoptosis in HCT116 cells. Further studies on the extract may also be investigated in future for the downregulation of cancer-related conditions to confirm its ability to prevent cancer.

## Acknowledgements

The author is grateful to the management of Annamalai University, Chidambaram, Tamil Nadu.

## Authors' contributions

MS performed the experiment and wrote the data. SV evaluated the data and reviewed the manuscript. All the authors read and approved the final manuscript.

## Compliance with ethical standards

**Conflict of interest:** Authors do not have any conflict of interests to declare.

**Ethical issues:** None

## References

1. Wai HK, Zainal Abidin SA, Othman I, Naidu R. Insights into the role of microRNAs in colorectal cancer (CRC) metabolism. Cancers (Basel). 2020;12(9):2462. https://doi.org/10.3390/cancers12092462
2. Deepa B, Babaji HV, Hosmani JV, Alamir AWH, Mushtaq S, Raj AT, et al. Effect of *Tinospora cordifolia*-derived phytocomponents on cancer: A systematic review. Appl Sci. 2019;9(23):5147. https://doi.org/10.3390/app9235147
3. Sharma B, Yadav A, Dabur R. Interactions of a medicinal climber *Tinospora cordifolia* with supportive interspecific plants trigger the modulation in its secondary metabolic profiles. Sci Rep. 2019;9:14327. https://doi.org/10.1038/s41598-019-50801-0
4. Tiwari P, Nayak P, Prusty SK, Sahu PK. Phytochemistry and pharmacology of *Tinospora cordifolia*: A review. Syst Rev Pharm. 2018;9(1):70–8. https://doi.org/10.5530/srp.2018.1.14
5. Prasad B, Chauhan A. Antioxidant and antimicrobial studies of *Tinospora cordifolia* (Guduchi/Giloy) stems and roots under *in vitro* condition. Int J Adv Microbiol Health Res. 2019;3(1):1–10.
6. Singh D, Chaudhuri PK. Chemistry and pharmacology of *Tinospora cordifolia*. Nat Prod Commun. 2017;12 (2):1934578X1701200240. https://doi.org/10.1177/1934578X1701200240
7. Sinha A, Sharma H, Singh B, Patnaik A. Phytochemical studies of methanol extracts of *Tinospora cordifolia* stem by GC–MS. World J Pharm Res. 2017;6(4):1319–26. https://doi.org/10.20959/wjpr20174-8205
8. Palmieri A, Scapoli L, Iapichino A, Mercolini L, Mandrone M, Poli F, et al. Berberine and *Tinospora cordifolia* exert a potential anticancer effect on colon cancer cells by acting on specific pathways. Int J Immunopathol Pharmacol. 2019;33:2058738419855567. https://doi.org/10.1177/2058738419855567
9. Shrestha T, Lamichhane J. Assessment of phytochemicals, antimicrobial, antioxidant and cytotoxicity activity of methanolic extract of *Tinospora cordifolia* (Gurjo). Nepal J Biotechnol. 2021;9 (1):18–23. https://doi.org/10.3126/njb.v9i1.38646
10. Sharma S, Mehmood Y, Sharma V, Kumar A, Kumar S, Bhat Z. Antioxidant potential of *Tinospora cordifolia*: Insights into its therapeutic significance. Int J Adv Biochem Res. 2024;8(2):425–7. https://doi.org/10.33545/26174693.2024.v8.i2Sf.616
11. Nyalo PO, Omwenga GI, Ngugi MP. Antibacterial properties and GC–MS analysis of ethyl acetate extracts of *Xerophyta spekei* (Baker) and *Grewia tembensis* (Fresen). Heliyon. 2023;9 (3):e14461. https://doi.org/10.1016/j.heliyon.2023.e14461
12. Abubakar AR, Haque M. Preparation of medicinal plants: Basic extraction and fractionation procedures for experimental purposes. J Pharm Bioallied Sci. 2020;12(1):1–10. https://doi.org/10.4103/jpbs.JPBS_175_19
13. Tamokou JD, Simo Mpetga DJ, Keilah Lunga P, Tene M, Tane P, Kuiate JR. Antioxidant and antimicrobial activities of ethyl acetate extract, fractions and compounds from stem bark of *Albizia adianthifolia* (Mimosoideae). BMC Complement Altern Med. 2012;12:99. https://doi.org/10.1186/1472-6882-12-99
14. Sellal A, Belattar R, Bouzidi A. Heavy metals chelating ability and antioxidant activity of *Phragmites australis* stems extracts. J Ecol Eng. 2019;20(2):116–23. https://doi.org/10.12911/22998993/96276

15. Hussen EM, Endalew SA. *In vitro* antioxidant and free-radical scavenging activities of polar leaf extracts of *Vernonia amygdalina*. BMC Complement Med Ther. 2023;23:146. https://doi.org/10.1186/s12906-023-03923-y

16. Ungureanu AR, Popovici V, Oprean C, Danciu C, Schroder V, Olaru OT, et al. Cytotoxicity analysis and in silico studies of three plant extracts with potential application in treatment of endothelial dysfunction. Pharmaceutics. 2023;15(8):2125. https://doi.org/10.3390/pharmaceutics15082125

17. Butt SS, Badshah Y, Shabbir M, Rafiq M. Molecular docking using Chimera and AutoDock Vina software for nonbioinformaticians. JMIR Bioinform Biotechnol. 2020;1(1):e14232. https://doi.org/10.2196/14232

18. Ononamadu CJ, Ibrahim A. Molecular docking and prediction of ADME/drug-likeness properties of potentially active antidiabetic compounds isolated from aqueous-methanol extracts of *Gymnema sylvestre* and *Combretum micranthum*. Biotechnologia. 2021;102(1):85–99. https://doi.org/10.5114/bta.2021.103765

19. Chi S, She G, Han D, Wang W, Liu Z, Liu B. Genus *Tinospora*: Ethnopharmacology, phytochemistry and pharmacology. Evid Based Complement Alternat Med. 2016;2016:9232593. https://doi.org/10.1155/2016/9232593

20. Sowmya M, Ramesh S, Ganne VS, Ramesh S, Jalantha P, Sujatha PL, et al. Phytochemical analysis of *Tinospora cordifolia* by GC–MS and evaluation of its antiurolithiatic potential by in silico. Indian Vet J. 2024;101(4):39–48. https://doi.org/10.62757/IVA.2024.101.4.39-48

21. Kashyap D, Agarwal T. Concentration and factors affecting the distribution of phthalates in the air and dust: A global scenario. Sci Total Environ. 2018;635:817–27. https://doi.org/10.1016/j.scitotenv.2018.04.158

22. Onoja J, Olawuni J. DPPH radical scavenging activity of corydine isolated from *Tinospora cordifolia*. Afr J Pharm Sci. 2023;3:68–78. https://doi.org/10.51483/AFJPS.3.2.2023.68-78

23. Boro A, Sujatha K, Abidharini JD, Pallavi P, Prabhu JPA, Anand AV. Evaluation of the antioxidative and qualitative properties of *Tinospora cordifolia*. Free Radic Antioxid. 2025;14(2):126–30. https://doi.org/10.5530/fra.2024.2.13

24. Polu PR, Nayanbhirama U, Khan S, Maheswari R. Assessment of free radical scavenging and anti-proliferative activities of *Tinospora cordifolia* Miers (Willd). BMC Complement Altern Med. 2017;17(1):457. https://doi.org/10.1186/s12906-017-1953-3

25. Kumar DV, Geethanjali B, Avinash KO, Kumar JR, Chandrashekrappa GK, Basalingappa KM. *Tinospora cordifolia*: The antimicrobial property of the leaves of Amruthaballi. J Bacteriol Mycol Open Access. 2017;5:147–56. https://doi.org/10.15406/jbmoa.2017.05.00147

26. Ezhilarasu K, Kasiranjan A, Priya S, Kamaraj A. The antibacterial effect of *Tinospora cordifolia* (Guduchi) and its role in combating antimicrobial resistance. Medeni Med J. 2023;38(3):149–58. https://doi.org/10.4274/MMJ.galenos.2023.84579

27. Patil S, Ashi H, Hosmani J, Almalki AY, Alhazmi YA, Mushtaq S, et al. *Tinospora cordifolia* (Thunb.) Miers (Giloy) inhibits oral cancer cells in a dose-dependent manner by inducing apoptosis and attenuating epithelial–mesenchymal transition. Saudi J Biol Sci. 2021;28(8):4553–9. https://doi.org/10.1016/j.sjbs.2021.04.056

28. Ali H, Dixit S. Extraction optimization of *Tinospora cordifolia* and assessment of the anticancer activity of its alkaloid palmatine. Sci World J. 2013;2013:1–10. https://doi.org/10.1155/2013/376216

29. Todsaporn D, Zubenko A, Kartsev VG, Mahalapbutr P, Geronikaki A, Sirakanyan SN, et al. Furopyridine derivatives as potent inhibitors of the wild type, L858R/T790M and L858R/T790M/C797S EGFR. J Phys Chem B. 2024;128(50):12389–402. https://doi.org/10.1021/acs.jpcb.4c06246

30. Ahmad K, Hafeez ZB, Bhat AR, Rizvi MA, Thakur SC, Azam A, et al. Antioxidant and apoptotic effects of *Callistemon lanceolatus* leaves and their compounds against human cancer cells. Biomed Pharmacother. 2018;106:1195–209. https://doi.org/10.1016/j.biopha.2018.07.016

31. Ren X, Zhang J, Dai A, Sun P, Zhang Y, Jin L, et al. Synthesis and biological evaluation of novel furopyridone derivatives as potent cytotoxic agents against esophageal cancer. Int J Mol Sci. 2024;25(17):9634. https://doi.org/10.3390/ijms25179634

## Additional information

**Peer review**: Publisher thanks Sectional Editor and the other anonymous reviewers for their contribution to the peer review of this work.

**Reprints & permissions information** is available at https://horizonepublishing.com/journals/index.php/PST/open_access_policy

**Publisher's Note**: Horizon e-Publishing Group remains neutral with regard to jurisdictional claims in published maps and institutional affiliations.

**Indexing**: Plant Science Today, published by Horizon e-Publishing Group, is covered by Scopus, Web of Science, BIOSIS Previews, Clarivate Analytics, NAAS, UGC Care, etcSee https://horizonepublishing.com/journals/index.php/PST/indexing_abstracting



**Publisher information:** Plant Science Today is published by HORIZON e-Publishing Group with support from Empirion Publishers Private Limited, Thiruvananthapuram, India.